IEEE Access
Multidisciplinary | Rapid Review | Open Access Journal

Received March 4, 2019, accepted March 18, 2019, date of publication April 9, 2019, date of current version April 19, 2019.

Digital Object Identifier 10.1109/ACCESS.2019.2909044

A New Droop Coefficient Design Method for Accurate Power-Sharing in VSC-MTDC Systems

YUCHAO LIU[1], TIM C. GREEN[2], (Fellow, IEEE), JIAN WU[1], KUMARS ROUZBEHI[3], (Senior Member, IEEE), ALI RAZA[4], AND DIANGUO XU[1], (Fellow, IEEE)

[1]Department of Electrical Engineering, Harbin Institute of Technology, Harbin 150001, China
[2]Department of Electrical and Electronic Engineering, Imperial College London, London SW7 2AZ, U.K.
[3]Department of Electrical Engineering, University of Seville, Seville 41092, Spain
[4]Department of Electrical Engineering, The University of Lahore, Lahore 55150, Pakistan

Corresponding author: Yuchao Liu (liuyuchaohit@outlook.com)

This work was supported in part by the National Natural Science Foundation of China under Grant 51720105008, and in part by the Open Fund of Operation and Control of Renewable Energy and Storage Systems.

ABSTRACT This paper proposes a new droop coefficient design method with the aim of improving the power-sharing accuracy among the converters in a multi-terminal dc (MTDC) system. The proposed droop coefficient design method works by adjusting the droop coefficient and can realize an arbitrary power-sharing ratio among all the converters in an MTDC system. This method does not rely on a communication network and therefore has the potential for higher reliability than the alternative methods. Mitigating the impact of the variation of dc line resistances on the power-sharing is discussed. Simulation of a four-terminal MTDC system is carried out by using PSCAD/EMTDC. The experimental results under a scaled-down four-terminal dc grid platform demonstrate the effectiveness of the proposed method.

INDEX TERMS VSC-MTDC system, accurate power-sharing, droop control, dc line resistance.

NOMENCLATURE

i, j	The subscripts *i*, *j* represent the *i*th and *j*th VSC station
u_{dc}^*, u_{dc}	The reference and measurement values of the dc voltage
Δu_{dc}, ΔP	The deviations of dc voltage and power
u_{dc0}	The dc voltage of the common node 0 between VSC1 and VSC2
i_{dc}	The dc current transferred between VSCs
R	The equivalent dc line resistance
r, r_v	The droop coefficient of the VSC and the equivalent virtual resistance of droop coefficient under *V-I* droop control
k	The *V-P* droop coefficient of the VSC
P^*, ΔP_{max}	The reference power and the maximum power variation
P_{WF},P, P_{max}	The output power of wind farms (WF), measured power of VSCs, and the maximum power transmission capacity

The associate editor coordinating the review of this manuscript and approving it for publication was Zhiyi Li.

I. INTRODUCTION

The development and growth of renewable energy sources distant from load centers has led to the need for HVDC connections [1], [2]. Compared with the traditional point-to-point HVDC systems, multi-terminal HVDC grids based on voltage source converters (VSC-MTDC) bring advantages such as higher reliability, better self-protection and greater operational flexibility [3], [4]. These advantages of VSC-MTDC make it a promising technology for integrating offshore wind farms (WF) with mainland grids, long distance bulk power delivery, and construction of future super grids [5], [6].

Droop-control and variants of it have been widely studied in MTDC systems because of its clear advantage of avoiding the need for high-speed communication links [8], [9]. Conventional droop-control methods can be classified into two broad categories. The first is current-mode droop which includes current-voltage (*I-V*) droop where current is varied as a function of observed dc voltage and power-voltage (*P-V*) droop where power is varied in response to dc voltage. The second is voltage-mode droop which includes dc voltage-current (*V-I*) and dc voltage-power (*V-P*) droop where voltage is varied in response to either current or power. Voltage-mode droop is the more commonly applied method in VSC-MTDC

systems because the dc voltage is an important indicator of stability of such system.

Droop control has the advantage of high reliability because it rests on local measurements only and avoids the vulnerability of high-speed communication links between terminals, but the disadvantage is that power-flow dispatch is not perfectly controlled [9], [11], [12]. Normally, there will be a mismatch between the voltages at the terminals of the VSCs, the size of which depends on the dc line resistances, the droop coefficients and any sensor gain errors [12]. As a result, differences in power-sharing between the VSCs will appear. In a dc microgrid, it is reasonable to assume that the line resistances are far smaller than the so-called virtual resistance that appears from the operation of the droop-control [13], and the effect of line resistance on the dc voltage deviation is small enough to be ignored. However, in the MTDC grids, the line resistances are relatively large such that they cannot be ignored and will significantly affect the accuracy of the power-sharing, most notably when the line resistances for the various terminals are significantly different [13].

Since the accuracy of power-sharing is affected by the dc line resistance and the deviation of the dc voltage, the output powers of VSCs are no longer strictly inversely proportional to their droop coefficients. In the worst case, imperfect power-sharing may lead to overloading of the VSC stations [14]. It is possible to use a relatively large droop coefficient to reduce the impact of the line resistance and improve the power-sharing but this causes a larger deviation of the dc voltage from its nominal value [15]. Thus, conventional droop controllers are not effective in achieving accurate power-sharing over long transmissions. Centralized control strategies can overcome this issue but high-bandwidth communication becomes crucial and is vulnerable to a single point failure, and thus is not a preferred solution [16].

In order to address the load sharing issue, various control methods have been proposed in the literature [11]–[13], [17]–[21]. In [11], the authors discussed the impact of dc line voltage drops on the power flow of MTDC using droop control. However, they neglected the impact of dc line resistance on both the dc current and droop coefficient. A basic secondary compensator was presented in [12]. It is applicable to systems where the voltage of a common dc bus voltage can be measured by a remote voltage sensor and therefore suits small microgrids not multi-terminal grids without a common bus. In [13], an improved droop control method for dc grids was proposed to enhance the current accuracy. However, this method is only applicable for current sharing in a microgrid. The method relies on communication, albeit at low bandwidth, but the effect of communication failure was not treated. To improve load-sharing performance, a distributed secondary control for proportional load sharing in low-voltage dc microgrids was proposed in [17]. It uses only a local controller and does not need any remote sensor, which means it effectively avoids the single-point vulnerability of a central controller. However, this method can only achieve current-sharing accuracy with large droop coefficients which in turn will cause larger dc voltage deviations. In [18], the authors combined dynamic averaging, voltage shifting and slope adjustment to implement an adaptive droop coefficient. In [19], the authors analyzed the impact of the droop coefficient setting and the dc grid topology on power-sharing between converters. A solution was presented to optimize the tradeoff between minimizing the power sharing errors and dc voltage errors.

The methods reviewed thus far were focused on overcoming the dc voltage deviation caused by the dc line resistance. However, they neglected the effect of the dc line resistance on the droop coefficients or dc current. In [21], the authors reviewed and compared several types of centralized and distributed secondary control methods. The methods of this type assumed that the resistance of a dc line can be accurately estimated from its length and datasheet specification of its conductors. However, the resistances are known to vary with operating conditions, notably temperature [22]. Changes in resistance and operational conditions have an effect on the droop coefficient [23]. In [24], an average dc voltage regulation method based on V-P control is proposed. It improved the power-sharing accuracy by regulating the dc voltage in all VSCs. However, communication was required between the VSC converters. Communications delays were neglected.

Despite the volume of work in the area, there is scope for improving power-sharing accuracy, particularly in MTDC grids, rather than dc microgrids, significant and different dc line resistance appear between the converters. This paper makes a proposal for such an improvement and is organized as follows: Section II presents the mathematical description of the *V-I* and *V-P* droop control. Later, the impact of the dc line resistance and droop coefficient on power-sharing is discussed. In Section III, the droop coefficient design method is proposed. Meanwhile, the impact of the dc line resistance variation on the power-sharing is analyzed and discussed. In Section IV, the simulation results are presented. Section V presents the experimental platform and results. Section VI concludes this paper.

II. MODELLING OF MTDC SYSTEM

A. VOLTAGE-CURRENT AND VOLTAGE-POWER DROOP CONTROL STRATEGIES

Two control schemes for voltage-mode droop-controlled VSC are depicted in Fig. 1, namely droop of voltage against current, *V-I,* and droop of voltage against power, *V-P*. The droop coefficients can be expressed according to the branch output current and output active power as shown in (1). It should be noted that the definition of the droop coefficient is presented in reciprocal form in some literature [6], [22], [24].

$$\begin{cases} r = \dfrac{\Delta u_{\mathrm{dc}}}{\Delta i_{\mathrm{dc}}} = \dfrac{u^*_{\mathrm{dc}} - u_{\mathrm{dc}}}{i^*_{\mathrm{dc}} - i_{\mathrm{dc}}} \\ k = \dfrac{\Delta P}{\Delta u_{\mathrm{dc}}} = \dfrac{P^* - P}{u^*_{\mathrm{dc}} - u_{\mathrm{dc}}} \end{cases} \tag{1}$$

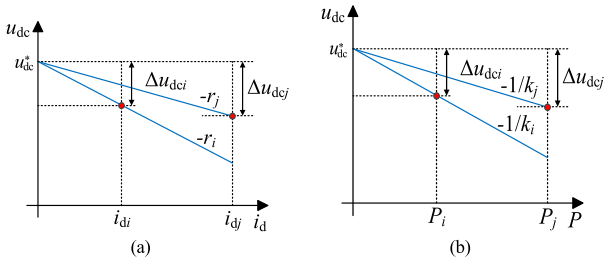

FIGURE 1. (a) V-I control mode. (b) V-P control mode.

Generally, *V-I* control can be based on either local voltage feedback (LVF) or global voltage feedback (GVF). However, GVF relies on being able to identify a common bus from which to take such feedback, which is not generally present in a MTDC system. For a set of parallel branches, the current sharing ratios for steady-state conditions can be derived as in (2) for LVF and GVF, respectively.

$$\begin{cases} i_{dc1} : i_{dc2} : \cdots : i_{dcn} = \dfrac{1}{(r_1 + R_1)} : \dfrac{1}{(r_2 + R_2)} \\ \qquad\qquad : \cdots \dfrac{1}{(r_n + R_n)} \\ i_{dc1} : i_{dc2} : \cdots : i_{dcn} = \dfrac{1}{r_1} : \dfrac{1}{r_2} : \cdots \dfrac{1}{r_n} \end{cases} \tag{2}$$

For *V-P* control mode, power-sharing ratios among the droop controlled parallel branches under ideal conditions (meaning u_{dci} are the same in each terminal) can be expressed as in (3).

$$\Delta P_1 : \Delta P_2 : \cdots : \Delta P_n = k_1 : k_2 : \cdots : k_n \tag{3}$$

In practice, due to the line resistance and dc voltage deviation, the VSCs do not behave rigidly according to the preset characteristics [26], which means the output powers of the VSCs are not inversely proportional to the droop coefficients. Various traditional methods such as [24], [25], attempt to compensate the voltage drop by regulating the dc voltage and thereby reduce the power-sharing error caused by the line resistance. However, the relationship between the power-sharing, the droop coefficient and the line resistance is rarely discussed.

B. MATHEMATICAL MODEL AND POWER-SHARING PERFORMANCE OF VOLTAGE-CURRENT DROOP CONTROL

In order to analyze the relationship between the power-sharing, the droop coefficient and the dc line resistance, a mathematical model of the *V-I* droop control is derived. A four-terminal MTDC system architecture under study in this paper is shown in Fig.2. The equivalent circuit of an arbitrary parallel MTDC system is shown in Fig. 3. The wind farms are modeled as controlled current sources with current of P_{WF}/u_{dc} set by the output power P_{WF}. The VSCs act as dc voltage sources which absorb power and their droop coefficient is shown as an equivalent virtual resistor r_i.

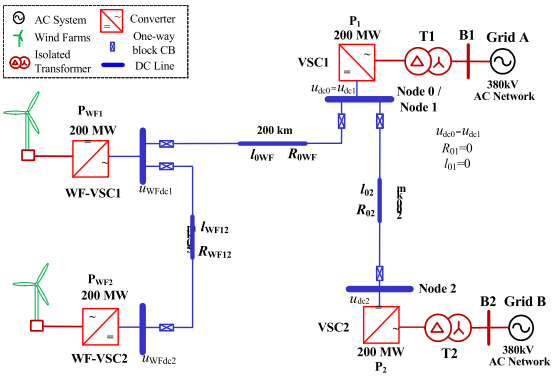

FIGURE 2. Four-terminal MTDC system architecture under study.

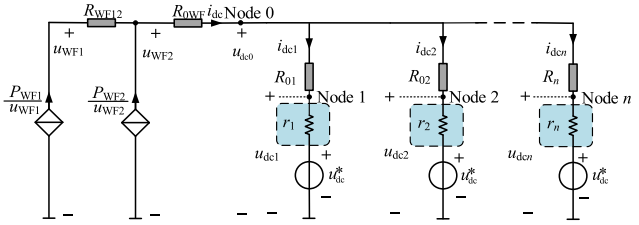

FIGURE 3. Simplified equivalent circuit of a MTDC system under V-I droop control.

The voltage expressions of the droop-controlled converters of Fig. 3 are given in (4). The dc voltage deviation between the reference value and the actual measurement of the dc voltage Δu_{dci} is expressed in (5).

$$u_{dc0} = u^*_{dc} + (R_{01} + r_1)i_{dc1} = u^*_{dc} + (R_{02} + r_2)i_{dc2} \tag{4}$$

$$\begin{bmatrix} \Delta u_{dc1} \\ \Delta u_{dc2} \\ \vdots \\ \Delta u_{dcn} \end{bmatrix} = \begin{bmatrix} u^*_{dc} \\ u^*_{dc} \\ \vdots \\ u^*_{dc} \end{bmatrix} - \begin{bmatrix} u_{dc1} \\ u_{dc2} \\ \vdots \\ u_{dcn} \end{bmatrix} = \begin{bmatrix} r_1 i_{dc1} \\ r_2 i_{dc2} \\ \vdots \\ r_n i_{dcn} \end{bmatrix} \tag{5}$$

Equation (4) shows that the dc currents in droop-controlled VSCs are inversely proportional to the resistances.

$$\frac{i_{dci}}{i_{dcj}} = \frac{R_{0j} + r_j}{R_{0i} + r_i} \tag{6}$$

According to (6), it can be observed that if and only if $R_{0i} = R_{0j} = 0$, is the dc current is inversely proportional to the droop coefficient. In realistic conditions, where the lines have resistance, the dc current is affected by both the dc line resistance and the droop coefficient. It is common in micro-gird analysis, where distances are short, to neglect the dc line resistance, however, in MTDC systems, the dc line resistances are expected to be significant and cannot be neglected. The analysis of the droop coefficient and dc line resistance in a MTDC system is reported in Section III.

Combining (5) and (6), the deviation in dc voltage between the VSCs can be obtained in (7).

$$\Delta u_{ij} = u_{dci} - u_{dcj} = r_i i_{dci} - r_j i_{dcj} = (r_i - r_j \frac{R_{0i} + r_i}{R_{0j} + r_j}) i_{dci} \tag{7}$$

From (7), it is concluded that the difference between the output voltage Δu_{dcij} will be zero only if $r_i/r_j = R_{0i}/R_{0j}$. Combining (4) and (5), the active power of the VSCs is obtained in (8).

$$\begin{bmatrix} P_1 \\ P_2 \\ \vdots \\ P_n \end{bmatrix} = \begin{bmatrix} u_{\mathrm{dc1}} i_{\mathrm{dc1}} \\ u_{\mathrm{dc2}} i_{\mathrm{dc2}} \\ \vdots \\ u_{\mathrm{dcn}} i_{\mathrm{dcn}} \end{bmatrix} = \begin{bmatrix} (u^*_{\mathrm{dc}} + r_1 i_{\mathrm{dc1}}) i_{\mathrm{dc1}} \\ (u^*_{\mathrm{dc}} + r_2 i_{\mathrm{dc2}}) i_{\mathrm{dc2}} \\ \vdots \\ (u^*_{\mathrm{dc}} + r_n i_{\mathrm{dcn}}) i_{\mathrm{dcn}} \end{bmatrix} \tag{8}$$

Combining (6) and (7), the deviation of the active power between converters can be expressed in (9).

$$\begin{aligned} \Delta P_{ij} &= P_i - P_j \\ &= u^*_{\mathrm{dc}}(1 - \frac{R_{0i} + r_i}{R_{0j} + r_j}) i_{\mathrm{dc}i} + [r_i - r_j(\frac{R_{0i} + r_i}{R_{0j} + r_j})^2] i^2_{\mathrm{dc}i} \end{aligned} \tag{9}$$

From (9), it can be observed that if and only if $R_{0i} = R_{0j}$ and $r_i = r_j$ will $P_i = P_j$, and the system power be evenly distributed between VSCi and VSCj, otherwise, the power-sharing accuracy is degraded. Obviously, as the cable routes are not identical, it is not possible to satisfy $R_{0i} = R_{0j}$ precisely even for line lengths that are nominally the same.

In the case of a V-I droop controller, the equivalent output resistances of the VSCs can be adjusted to give $R_{0i} + \mathrm{r}_i = R_{0j} + \mathrm{r}_j$ to maintain the current-sharing. By substituting $R_{0i} + \mathrm{r}_i = R_{0j} + \mathrm{r}_j$ into (9), the active power deviation in (9) can be rewritten as

$$\Delta P_{ij} = (r_i - r_j) i^2_{\mathrm{dc}i} \tag{10}$$

According to (10), there is a power-sharing error between two VSCs even when output resistances are equal. Hence, the methods which regulate the output resistance proportion based on the V-I droop control to realize proportional current-sharing are not applicable to the V-P droop-based power-sharing.

III. PROPOSED OPTIMIZED DROOP COEFFICIENT DESIGN MEHTOHD

A. PROPOSED DROOP COEFFICIENT DESIN METHOD UNDER VOLTAGE-POWER DROOP CONTROL STRATEGIES

The method of analysis used for V-I droop can now be applied to V-P droop control and the relationship between power-sharing, the droop coefficient and the dc line resistance identified. From there methods for V-P control can be derived.

The power variation of a converter can be expressed as:

$$\Delta P_i = (u^*_{\mathrm{dc}} + \Delta u_{\mathrm{dc}i})(i^*_{\mathrm{dc}i} + \Delta i_{\mathrm{dc}i}) - u^*_{\mathrm{dc}} i^*_{\mathrm{dc}i} \tag{11}$$

This can be approximated by neglecting the second-order term and, for a V-P droop, can be equated to the voltage deviation multiplied by the droop gain, k, as shown in (12).

$$\Delta P_i \approx i^*_{\mathrm{dc}i} \Delta u_{\mathrm{dc}i} + u^*_{\mathrm{dc}} \Delta i_{\mathrm{dc}i} \approx k_i \Delta u_{\mathrm{dc}i} \tag{12}$$

Re-arranging (12) reveals the equivalent virtual resistor, r_{v}, that exists under V-P droop-control (which is similar to that under V-I droop-control), as shown in (13).

$$r_{\mathrm{v}i} = \frac{\Delta u_{\mathrm{dc}i}}{\Delta i_{\mathrm{dc}i}} = \frac{u^*_{\mathrm{dc}}}{k_i - i^*_{\mathrm{dc}i}} \tag{13}$$

Then the improved equivalent circuit of an arbitrary parallel MTDC system under V-P control can be simplified to the circuit shown in Fig. 4.

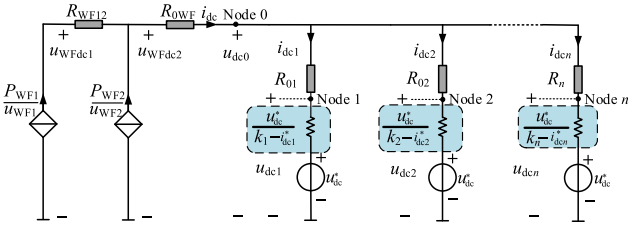

FIGURE 4. Improved equivalent circuit of MTDC system under V-P droop control.

The maximum droop coefficient is restricted by the power transmission capacity and the allowable dc voltage deviation (for instance, no more than 5%). The range of the droop coefficient value can be expressed as

$$k \geq P_{\max} / \Delta u_{\mathrm{dc\,max}} \tag{14}$$

where, $\Delta u_{\mathrm{dc\,max}} = 5\% \times u^*_{\mathrm{dc}}$ is the maximum dc voltage deviation. From (14), we can observe that in order to reduce the dc voltage deviation, a larger droop coefficient should be selected. However, we see from (13), that the larger the droop coefficient k_i, the smaller the virtual resistance $r_{\mathrm{v}i}$, which means the dc line resistance has a great impact on the current-sharing among the VSCs as given in (6).

To explore this further we take an example in which the power transmission capacity of the system is $P_{\max}$ =200 MW and the dc voltage reference value is $u^*_{\mathrm{dc}} = 200$ kV, then the maximum dc current is $i_{\mathrm{dcmax}} = P_{\max}/u^*_{\mathrm{dc}} = 1$ kA. According to (14), the minimum droop coefficient k is obtained as 20 MW/kV. By converting the droop coefficient k into the form of (13), the limit on the virtual resistance can be obtained as $r_{\mathrm{v}} \leq 10.52$. The length of the dc line in this example is 200 km and a typical value of resistivity of a dc line is 0.02 Ω/km [25] and so the total line resistance is set at $R = 4$ Ω. Obviously, a line resistance of 4 Ω cannot be ignored in comparison to the maximum virtual resistance r_{v} of 10.52 Ω, which is implied by the minimum droop coefficient.

From (11), the power-sharing deviation P_{ij} between VSCi and VSCj P_{ij} can be expressed as

$$\Delta P_{ij} = \Delta P_i - \Delta P_j = k_i \Delta u_{\mathrm{dc}i} - k_j \Delta u_{\mathrm{dc}j} \tag{15}$$

Combining (5), (6) and (13), (15) results:

$$\Delta P_{ij} = \frac{u^*_{\mathrm{dc}} i_{\mathrm{dc}i}}{k_i - i^*_{\mathrm{dc}i}} \left[k_i - k_j \frac{R_{01}(k_i - i^*_{\mathrm{dc}i}) + u^*_{\mathrm{dc}}}{R_{02}(k_j - i^*_{\mathrm{dc}j}) + u^*_{\mathrm{dc}}} \right] \tag{16}$$

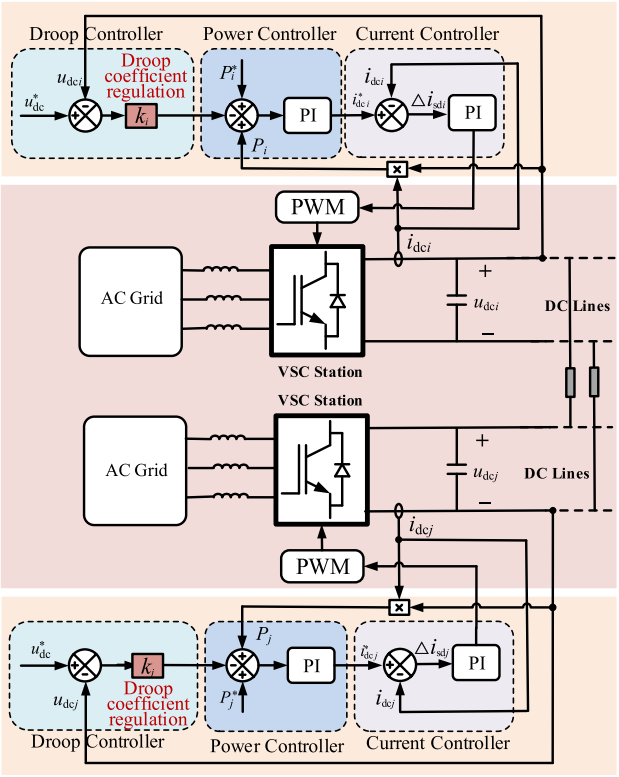

FIGURE 5. Block diagram of a voltage-mode (V-P) controlled VSC-MTDC system with the proposed droop design method.

Define $f(k) = k_i - k_j \left[\frac{R_{01}(k_i - i^*_{dci}) + u^*_{dc}}{R_{02}(k_j - i^*_{dcj}) + u^*_{dc}}\right]$. We can obtain that if $f(k) = 0$ is satisfied, then the power sharing between VSCi and VSCj will be equal.

Similarly, the proportion of power sharing between VSCi and VSCj can be obtained as

$$\frac{\Delta P_i}{\Delta P_j} = \frac{k_i}{\left[k_j \frac{R_{0i}(k_i - i^*_{dci}) + u^*_{dc}}{R_{0j}(k_j - i^*_{dcj}) + u^*_{dc}}\right]} \tag{17}$$

$$k_j = \frac{D_j k_i}{D_i \frac{R_{0i}(k_i - i^*_{dci}) + u^*_{dc}}{R_{0j}(k_j - i^*_{dcj}) + u^*_{dc}}} \tag{18}$$

Therefore, the droop coefficients can be designed according to (18) for arbitrary proportional power sharing. Use of (18), requires for each converter only the initial reference dc voltage u^*_{dc}, the initial reference dc current i^*_{dc} and dc line resistance. No real-time information needs to be exchanged between the converters and so vulnerability to communication system interruptions or failures is removed. The control diagram of a V-P controlled VSC-MTDC system incorporating the proposed droop design method is shown in Fig.5. It includes the droop controllers, power controllers and current controllers. The proposed droop design method with droop coefficient regulation requires changes to the droop controller only.

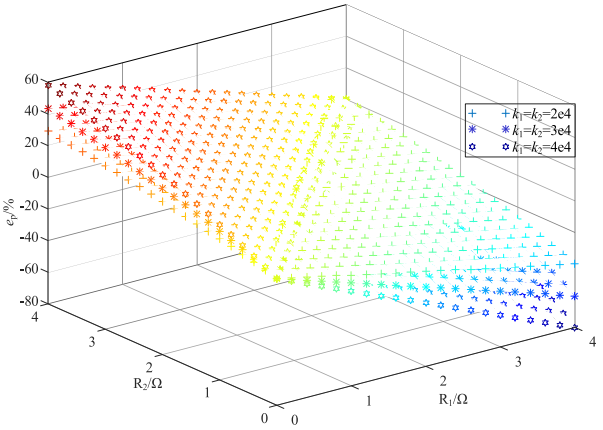

FIGURE 6. Power-sharing errors under different line resistances and droop coefficients with the traditional droop control.

B. COMPARISON OF POWER-SHARING ERROR WITHOUT AND WITH THE PROPOSED DROOP COEFFICIENT DESIGN METHOD

To compare the improvement in power-sharing (with the error being defined as $e_p = (P_1\text{-}P_2)/P_i^{**}100\%$), a test system was formed with the parameters in Table 5 and analyzed. Fig. 6 shows the power-sharing error e_p that was found under the traditional droop control with three choices of droop coefficients (the same being applied to VSC1 and VSC2 in each case) and plotted for ranges of line resistances. It can be seen that as the droop coefficients increase, the power sharing error will increase and the impact of dc line resistance on power sharing is large, too large to be neglected in a MTDC system. Moreover, as the droop coefficients decrease, the dc voltage deviation increases, as is expected from (14). It is apparent that there is a tradeoff between the dc voltage deviation and the power-sharing error.

TABLE 1. Power-sharing errors without the proposed droop coefficient design method under different dc line resistances ($k_1 = k_2 = 20$ MW/kV).

e_P(%)	R_{02}=0 Ω	R_{02}=1 Ω	R_{02}=2 Ω	R_{02}=3 Ω	R_{02}=4 Ω
R_{01}=0 Ω	0	9.11	16.76	23.29	28.91
R_{01}=1 Ω	9.97	0	8.38	15.53	21.68
R_{01}=2 Ω	19.95	9.11	0	7.76	14.46
R_{01}=3 Ω	29.92	18.22	8.38	0	7.23
R_{01}=4 Ω	39.90	27.33	16.76	7.76	0

For ease of reference, selected results for power-sharing error e_p are repeated in Table 1. As Table 1 reveals, without the proposed droop coefficient regulation, the power-sharing error e_p increases as the difference between resistances R_{01} and R_{02} of the lines and is only zero if R_{01} is equal to $R_{02,}$.

To apply the proposed droop design method, the droop coefficient for VCS1 was set at $k_1 = 20$ MW/kV. The coefficient for VSC2, was then k_2 adjusted according to the dc line resistances R_{01} and R_{02}. The updated droop coefficients k_2 are given in Table 2. With the proposed droop coefficient design method, the power-sharing errors e_p were maintained at zero

TABLE 2. Updated droop coefficient k_2 with the proposed droop coefficient design method under different dc line resistances (k_1 = 20 MW/kV).

k_2(MW/kV)	R_{02}=0 Ω	R_{02}=1 Ω	R_{02}=2 Ω	R_{02}=3 Ω	R_{02}=4 Ω
R_{01}=0 Ω	20	22.2222	25	28.5714	33.3333
R_{01}=1 Ω	18.1818	20	22.2222	25	28.5714
R_{01}=2 Ω	16.6667	18.1818	20	22.2222	25
R_{01}=3 Ω	15.3846	16.6667	18.1818	20	22.2222
R_{01}=4 Ω	14.2857	15.3846	16.6667	18.1818	20

TABLE 3. Maximum absolute power sharing errors under ±10% variation in different dc line resistance without the proposed droop coefficient design method ($k_1 = k_2$ = 20 MW/kV).

e_P(%)	R_{02}=0 Ω	R_{02}=1 Ω	R_{02}=2 Ω	R_{02}=3 Ω	R_{02}=4 Ω
R_{01}=0 Ω	0	9.85	18.01	24.89	30.75
R_1=1 Ω	10.87	1.75	10.58	18.04	24.4
R_1=2 Ω	21.75	11.96	3.24	11.19	18.06
R_1=3 Ω	32.62	21.78	12.52	4.53	11.71
R_1=4 Ω	43.49	31.80	21.81	13.18	5.65

TABLE 4. Maximum absolute power sharing errors under ± 10% variation in different dc line resistance with the proposed droop coefficient design method (k_1 = 20 mw/kv, the corresponding k_2 are presented in Table 2).

e_P(%)	R_{02}=0 Ω	R_{02}=1 Ω	R_{02}=2 Ω	R_{02}=3 Ω	R_{02}=4 Ω
R_{01}=0 Ω	0	1.01	2.06	3.14	4.25
R_{01}=1 Ω	0.91	1.75	2.70	3.69	4.70
R_{01}=2 Ω	1.68	2.42	3.24	4.15	5.07
R_{01}=3 Ω	2.33	3.01	3.70	4.53	5.39
R_{01}=4 Ω	2.90	3.52	4.14	4.87	5.65

TABLE 5. Designed system parameters for simulation.

Symbol	Name of parameters	Value
u_{dc}^*	Nominal reference direct voltage (kV)	400 (1 p.u.)
P_{base}	Active power base value (MW)	200
R_i	Equivalent resistance in ac side (Ω)	26
L_i	Equivalent inductance in ac side (mH)	72.4
C	DC capacitance (μF)	700
R_{line}	Resistance of the dc line (Ω/km)	0.005
L_{line}	Inductance of the dc line (mH/km)	0.16
C_{line}	Capacitance of the dc line (μF/km)	0.23
l_{WF12}	Length of the dc line (km)	50
l_{0WF}	Length of the dc line (km)	200
l_{01}	Length of the dc line (km)	200

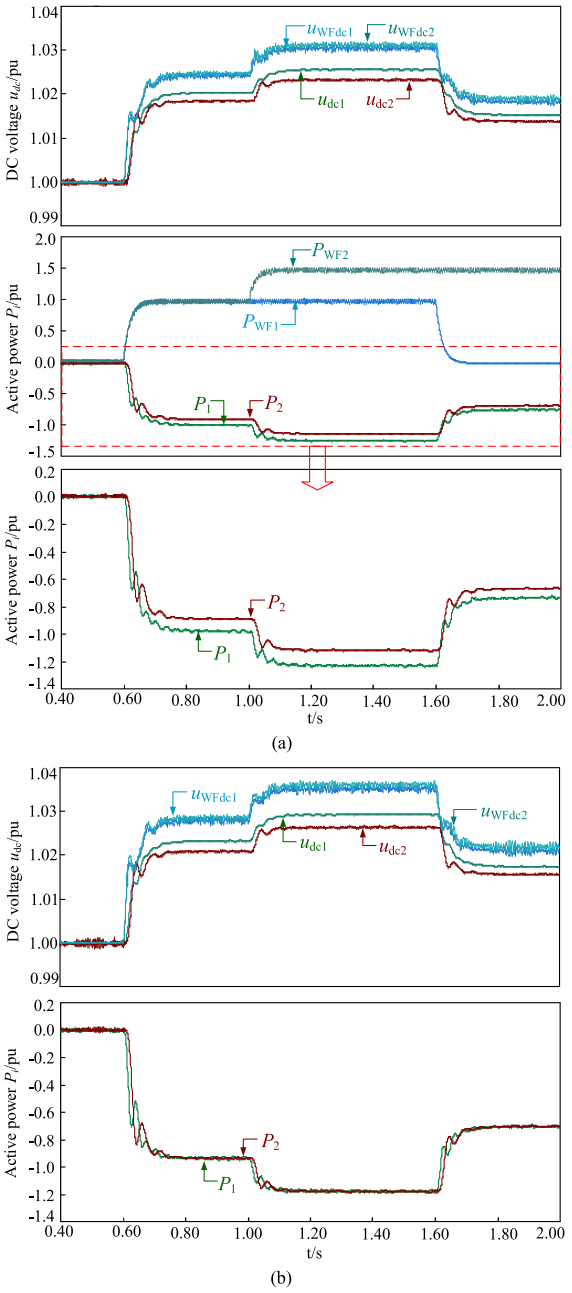

FIGURE 7. (a) Simulation results without the proposed droop coefficient design method ($k_1 = k_2$ = 20 MW/kV). (b) Simulation results with the proposed droop coefficient design method (k_1 = 20 MW/kV and k_2 = 22.22 MW/kV).

for various dc line resistance value, as expected from (18), provided the line resistances were accurately known.

C. IMPACT OF VARIATION OF DC LINE RESISTANCE ON POWER-SHARING

Since resistances of the dc lines vary with temperature, the estimated value of the dc resistance from the line length and data sheet values are not sufficiently accurate for practical application and better identification is needed. It can be expected from [21] that a basic real-time model of the cables would be able to estimate the core conductor resistance to within ±10%. That is taken as a guide here and power sharing is tested for variations of ±10% between the resistance values assumed in the controller and those in the network. For the test that follows, line resistances R_{01} and R_{02} are each varied in 1% steps from −10% to +10% are applied to the onshore VSCs, giving 20 × 20 combinations of R_{01} and R_{02}. The maximum absolute power-sharing errors found when testing these combinations were recorded. Table 3 gives the results for standard droop control and Table 4 gives results for the proposed droop coefficient design. The condition $R_{01} = R_{02}$ gives the same power-sharing errors for the two controllers, which is consistent with the analysis in Section II.

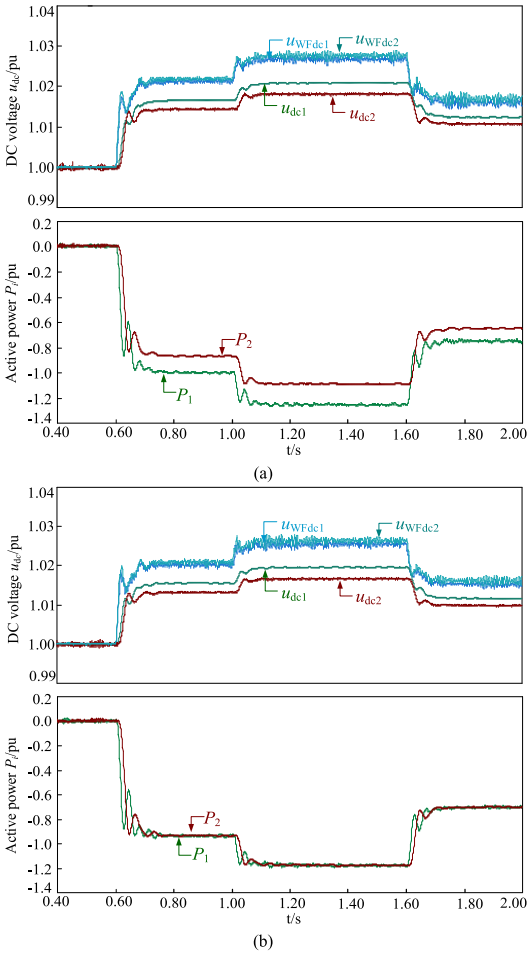

FIGURE 8. (a) Simulation results without the proposed droop coefficient design method ($k_1 = k_2 = 40$ MW/kV). (b) Simulation results with the proposed droop coefficient design method ($k_1 = 40$ MW/kV and $k_2 = 50$ MW/kV).

For unequal nominal resistances, the power-sharing errors are significantly improved by the proposed adjustment of the droop coefficients, more so for larger differences in line resistance between the VSCs.

IV. CASE STUDIES AND DYNAMIC SIMULATIONS

This case study will explore through dynamic simulation a four-terminal MTDC system as shown in Fig. 2. Two WFs are interfaced via WF-VSC1 and WF-VSC2 and controlled in active and reactive power control mode to inject power without contributing to the dc voltage regulation. Two converter stations, VSC1 and VSC2, will export power to a host AC system. Both are droop controlled to regulate the dc voltage and active power. In the following, the differences between the *V-I* and the *V-P* droop control modes are explained. A mathematical model is derived and used to analyze the power-sharing performance of *V-I* droop control. The parameters of the VSCs, dc lines and controller are listed in Table 5. For convenience, the values of the dc-link voltages and powers are presented in per-unit (p.u.).

TABLE 6. Comparison of simulation results under different scenarios (before: $k_1 = k_2 = 40$, after: $k_1 = 40$, $k_2 = 50$, unit: p.u.).

Scenarios			u_{dc1}	u_{dc2}	P_1	P_2	$\triangle P_{12}$
t=0.6~1s	Estimated dc line	before	1.0166	1.0145	1	0.870	0.13
		after	1.0157	1.0133	0.935	0.935	0
	10% variation	before	1.0170	1.0145	1	0.865	0.135
		after	1.0160	1.0130	0.950	0.930	0.02
	-10% variation	before	1.0167	1.0146	1	0.880	0.12
		after	1.0155	1.0135	0.935	0.945	-0.01
t=1~1.6s	Estimated dc line	before	1.0210	1.0184	1.260	1.100	0.16
		after	1.0197	1.0167	1.175	1.175	0
	10% variation	before	1.021	1.018	1.260	1.085	0.175
		after	1.020	1.017	1.190	1.170	0.02
	-10% variation	before	1.021	1.0185	1.250	1.100	0.15
		after	1.019	1.0175	1.170	1.185	-0.015
t=1.6~2s	Estimated dc line	before	1.0135	1.011	0.760	0.555	0.205
		after	1.0188	1.010	0.700	0.700	0
	10% variation	before	1.0127	1.0108	0.760	0.645	0.115
		after	1.0112	1.0083	0.710	0.700	0.01
	-10% variation	before	1.0125	1.011	0.750	0.650	0.10
		after	1.0112	1.0107	0.700	0.710	-0.01

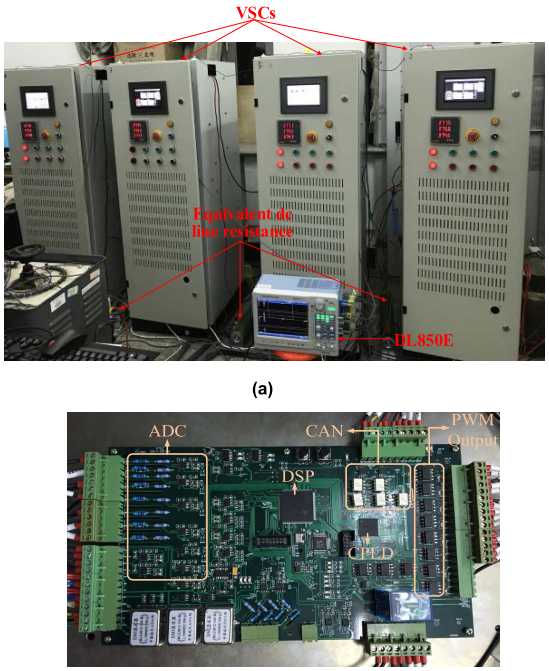

FIGURE 9. Experimental platform of the four-terminal VSC-MTDC. (a) Platform of four-terminal VSC-MTDC. (b) Main control board.

Using the dc line parameters in Table 5, the values estimated for the dc line resistance R_{01} and R_{02} when considered in the format of Fig. 3 are 0 Ω and 1 Ω, respectively. Three tests are formulated as described in the following (a), (b) and (c) sub-sections.

(a) At $t = 0.6$ s, the WFs start to inject power ($P_{WF1} = P_{WF2} = 1.0$ p.u.) into the grid.
(b) At $t = 1.0$ s, the power generated by WF-VSC2 increases from 1 p.u. to 1.5 p.u..
(c) At $t = 1.6$ s, WF-VSC1 disconnects from the system.

The simulation results are shown in Fig. 7 for cases without and with the proposed droop coefficient design method and then again and Fig. 8 for a different choice of droop coefficient, as noted in the captions. In order to observe

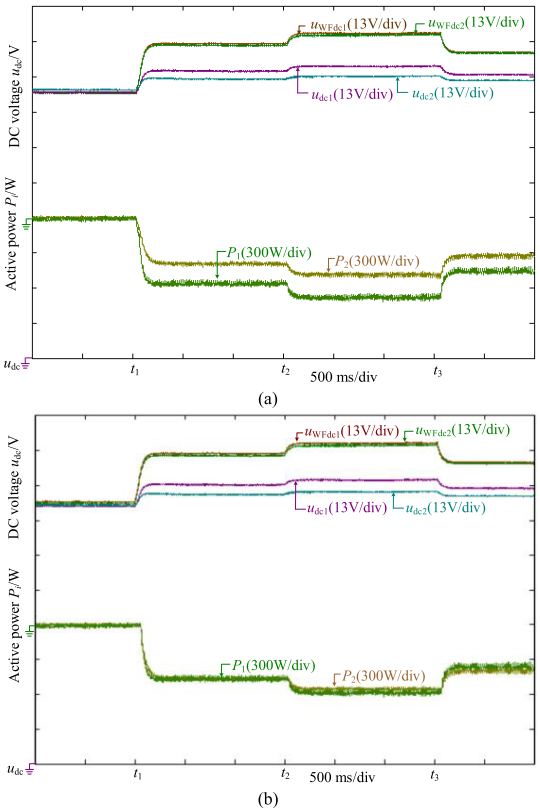

FIGURE 10. Experimental results (a) without the proposed droop coefficient design method ($k_1 = k_2 = 40$ W/V) and (b) with the proposed droop coefficient design method ($k_1 = 40$ W/V and $k_2 = 66.67$ W/V).

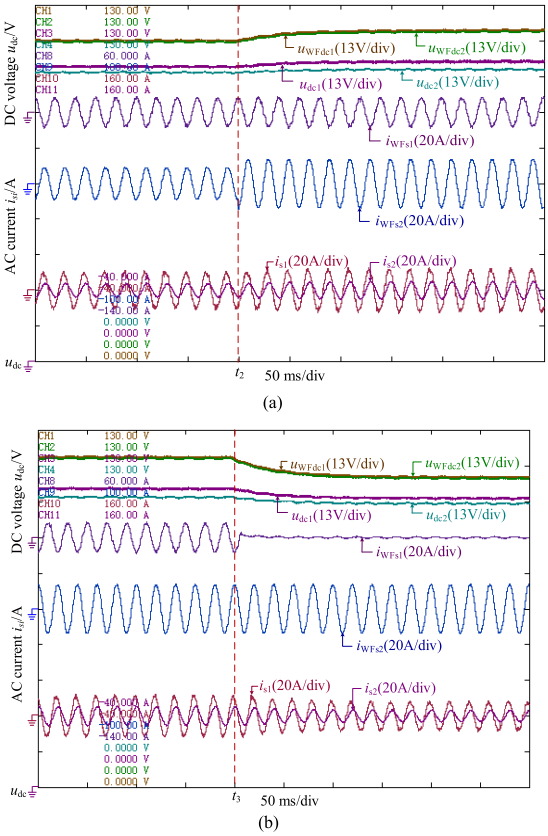

FIGURE 11. Experimental results without the proposed droop coefficient design method ($k_1 = k_2 = 40$ W/V). (a) Active power of WF-VSC2 step changes from 0.6 kW to 0.9 kW at t= t_2. (b) WF-VSC2 disconnects from the grid at t= t_3.

the power tracking more clearly, P_1 and P_2 are also shown zoomed in for the region between the red dotted lines. As the dynamics of the two WFs are the same, only the active power of VSC1 and VSC2 are presented in the following simulation results. Looking first at systems without the proposed method, it is clear that with higher droop coefficients, Fig. 8(a) compared to Fig. 7(a), the dc voltage deviation is reduced but the deviation in power-sharing is increased. For the proposed droop coefficient design method, the droop coefficient k_1 is kept unchanged and k_2 is adjusted according to (17). As shown in Fig. 7(b) and Fig. 8(b), the power-sharing accuracy is improved.

An additional test with $\pm 10\%$ dc line resistance variation was conducted. With $\pm 10\%$ dc line resistance variation is difficult to observe the difference of the dc voltage and power in time-domain figures. Instead, the changes of dynamic changes between the standard and proposed controller are summarized in Table 6. From the comparison in Table 6, not only the power-sharing accuracy is significantly improved, but also the dc voltage deviation is reduced. From Fig. 7(a) and Fig. 8(a), as analyzed in Section II, VSC2 processed less power than VSC1 as the existence of the dc line resistance when the power changes dynamically. After the droop coefficient k_2 is adjusted, the power taken by VSC1 and VSC2 are almost equal. Even $\pm 10\%$ dc line resistance variation is added, the power-sharing error is almost negligible. It is proved that the proposed droop coefficient design method has good performance on improving power-sharing accuracy.

V. EXPERIMENTAL RESULTS

For further evaluation of the proposed control methods, a scaled-down laboratory setup of a four-terminal dc system was used. The ac-side filter inductance and resistance, and dc link capacitance of each VSC are 1.2 mH and 1.58 Ω, and 2.8 mF. The nominal dc voltage reference is 100 V. Each converter is controlled by a control board incorporating a TMS320F28335 as shown in Fig. 8. WF-VSC1 and WF-VSC2 are P-Q control, while VSC1 and VSC2 are droop controlled. The dc line resistance $R_1 = 0\ \Omega$ and $R_2 = 1\ \Omega$. The experimental results are recorded by YOKOGAWA DL850E.

The experimental results without and with the proposed droop coefficient design method are shown in Fig.10. At $t = t_1$, WFs start to inject 0.6 kW into the dc system. At $t = t_2$, the active power of WF2 is increased from 0.6 kW to 0.9 kW. At $t = t_3$, the WF1 disconnects from the grid. The original droop coefficients of k_1 and k_2 are both set as 40 W/V. However, there is power-sharing mismatch between P_1 and P_2 as the different dc line resistance, as shown in Fig. 10(a). As shown in Fig. 10(b), the power-sharing mismatch is

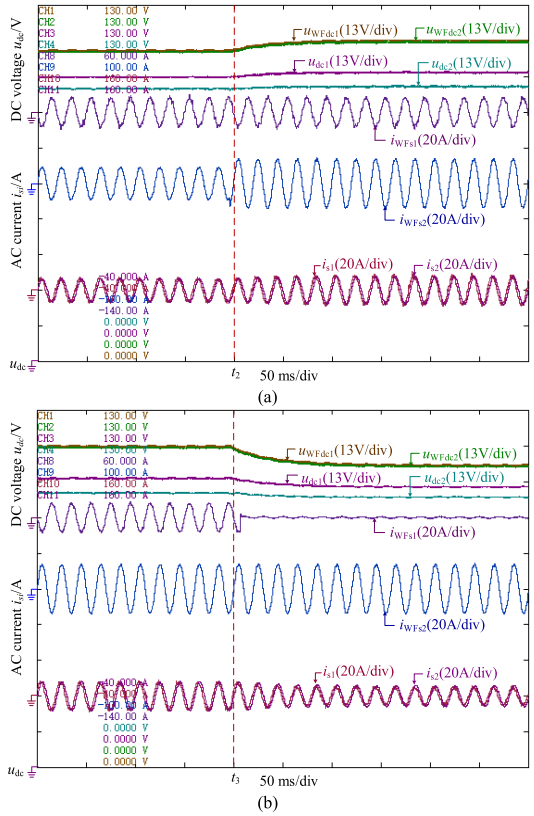

FIGURE 12. Experimental results with the proposed droop coefficient design method ($k_1 = 40$ W/V and $k_2 = 66.67$ W/V). (a) Active power of WF-VSC2 step changes from 0.6 kW to 0.9 kW at $t = t_2$. (b) WF-VSC2 disconnects from the grid at $t = t_3$.

eliminated by the proposed droop coefficient design method. During the comparison, k_1 is kept constant, while k_2 is updated according to (18).

To better illustrate the ability of the proposed method, the ac current experimental results of each VSC are recorded and compared. The ac voltage u_{sdi} of each VSC is set to be the same during each of the experimental case. According to $P_i = 1.5\, u_{sdi} i_{sdi}$, the ac current of each VSC i_{sdi} could also reflect the ac power of each VSC. Therefore, the ac current i_{WF1}, i_{WF2}, i_{s1}, i_{s2} of WF-VSC1, WF-VSC2, VSC1, and VSC2 under different scenarios are shown in Fig. 11 and Fig. 12, respectively. The experimental results of ac current and dc voltage of each VSC without the proposed droop coefficient design method under two dynamics are shown in Fig. 11(a) and (b), respectively. From Fig. 11, there is mismatch between i_{s1} and i_{s2} even the droop coefficients are set the same which is consistent with Fig. 10. The experimental results of ac current and dc voltage of each VSC with the proposed droop coefficient design method under two dynamic cases are shown in Fig. 12(a) and (b), respectively. From the comparison of Fig.11 and Fig.12, the mismatch of i_{s1} and i_{s2} caused by the difference of dc line resistance is well compensated by the proposed method. Hence, all the experimental results show that the accuracy of the power-sharing under the proposed method is significantly improved.

VI. CONCLUSIONS

In this paper, a new design method for droop coefficient regulation of VSC-MTDC systems is proposed. The proposed droop coefficient design method is intended to reduce or eliminate the mismatch of the effective droop coefficients caused by the resistance of the dc lines. The impact of variation of the dc line resistance, such as thermal variation, on the power-sharing under the proposed method is discussed. It is demonstrated that the proposed droop coefficient design method has good performance in terms of the power-sharing accuracy even under variation of the dc line resistance. The droop coefficient design method is implemented in the local VSC stations as part of a distributed control strategy that does not rely on any communication network and therefore avoids vulnerability to communication failures. Results from both a simulation case-study and a scaled-down experimental systems were verify the improvement of the power-sharing under the proposed control method.

REFERENCES

[1] T. Ackermann, "Transmission systems for offshore wind farms," *IEEE Power Eng. Rev.*, vol. 22, no. 12, pp. 23–27, Dec. 2002.
[2] P. Bresesti, W. L. Kling, R. L. Hendriks, and R. Vailati, "HVDC connection of offshore wind farms to the transmission system," *IEEE Trans. Energy Convers.*, vol. 22, no. 1, pp. 37–43, Mar. 2007.
[3] K. Rouzbehi, A. Miranian, A. Luna, and P. Rodriguez, "DC voltage control and power sharing in multiterminal DC grids based on optimal DC power flow and voltage-droop strategy," *IEEE J. Emerg. Sel. Topics Power Electron.*, vol. 2, no. 4, pp. 1171–1180, Dec. 2014.
[4] A. Raza, X. Dianguo, L. Yuchao, S. Xunwen, B. W. Williams, and C. Cecati, "Coordinated operation and control of VSC based multiterminal high voltage DC transmission systems," *IEEE Trans. Sustain. Energy*, vol. 7, no. 1, pp. 364–373, Jan. 2016.
[5] P. Rodriguez and K. Rouzbehi, "Multi-terminal DC grids: Challenges and prospects," *J. Mod. Power Syst. Clean Energy*, vol. 5, no. 4, pp. 515–523, 2017.
[6] Z. D. Wang *et al.*, "A coordination control strategy of voltage-source-converter-based MTDC for offshore wind farms," *IEEE Trans. Ind. Appl.*, vol. 51, no. 4, pp. 2743–2752, Jul./Aug. 2015.
[7] K. Rouzbehi, A. Miranian, J. I. Candela, A. Luna, and P. Rodriguez, "A generalized voltage droop strategy for control of multiterminal DC grids," *IEEE Trans. Ind. Appl.*, vol. 51, no. 1, pp. 607–618, Jan./Feb. 2015.
[8] W. Wang, Y. Li, Y. Cao, U. Häger, and C. Rehtanz, "Adaptive droop control of VSC-MTDC system for frequency support and power sharing," *IEEE Trans. Power Syst.*, vol. 33, no. 2, pp. 1264–1274, Mar. 2018.
[9] N. R. Chaudhuri and B. Chaudhuri, "Adaptive droop control for effective power sharing in multi-terminal DC (MTDC) Grids," *IEEE Trans. Power Syst.*, vol. 28, no. 1, pp. 21–29, Feb. 2013.
[10] F. Gao *et al.*, "Comparative stability analysis of droop control approaches in voltage-source-converter-based DC microgrids," *IEEE Trans. Power Electron.*, vol. 32, no. 3, pp. 2395–2415, Mar. 2017.
[11] T. M. Haileselassie and K. Uhlen, "Impact of DC line voltage drops on power flow of MTDC using droop control," *IEEE Trans. Power Syst.*, vol. 27, no. 3, pp. 1441–1449, Aug. 2012.
[12] S.-A. Amamra, F. Colas, X. Guillaud, P. Rault, and S. Nguefeu, "Laboratory demonstration of a multiterminal VSC-HVDC power grid," *IEEE Trans. Power Del.*, vol. 32, no. 5, pp. 2339–2349, Oct. 2017.
[13] X. Lu, J. M. Guerrero, K. Sun, and J. C. Vasquez, "An improved droop control method for dc microgrids based on low bandwidth communication with DC bus voltage restoration and enhanced current sharing accuracy," *IEEE Trans. Power Electron.*, vol. 29, no. 4, pp. 1800–1812, Apr. 2014.
[14] Y. Huang and C. K. Tse, "Circuit theoretic classification of parallel connected DC–DC converters," *IEEE Trans. Circuits Syst. I, Reg. Papers*, vol. 54, no. 5, pp. 1099–1108, May 2007.
[15] J. Ma, L. Yuan, Z. Zhao, and F. He, "Transmission loss optimization-based optimal power flow strategy by hierarchical control for DC microgrids," *IEEE Trans. Power Electron.*, vol. 32, no. 3, pp. 1952–1963, Mar. 2016.

[16] C. Gavriluta, R. Caire, A. Gomez-Exposito, and N. Hadjsaid, "A distributed approach for OPF-based secondary control of MTDC systems," *IEEE Trans. Smart Grid*, vol. 9, no. 4, pp. 2843–2851, Jul. 2018.
[17] J. M. Guerrero, J. C. Vasquez, J. Matas, L. G. de Vicuna, and M. Castilla, "Hierarchical control of droop-controlled AC and DC microgrids—A general approach toward standardization," *IEEE Trans. Ind. Electron.*, vol. 58, no. 1, pp. 158–172, Jan. 2011.
[18] S. Anand, B. G. Fernandes, and J. Guerrero, "Distributed control to ensure proportional load sharing and improve voltage regulation in low-voltage DC microgrids," *IEEE Trans. Power Electron.*, vol. 28, no. 4, pp. 1900–1913, Apr. 2013.
[19] J. Beerten and R. Belmans, "Analysis of power sharing and voltage deviations in droop-controlled DC grids," *IEEE Trans. Power Syst.*, vol. 28, no. 4, pp. 4588–4597, Nov. 2013.
[20] V. Nasirian, S. Moayedi, A. Davoudi, and F. L. Lewis, "Distributed cooperative control of DC microgrids," *IEEE Trans. Power Electron.*, vol. 30, no. 4, pp. 2288–2303, Apr. 2015.
[21] P. Wang, X. Lu, X. Yang, W. Wang, and D. G. Xu, "An improved distributed secondary control method for DC microgrids with enhanced dynamic current sharing performance," *IEEE Trans. Power Electron.*, vol. 31, no. 9, pp. 6658–6673, Sep. 2016.
[22] T. M. Haileselassie, A. G. Endegnanew, and K. Uhlen, "Secondary control in multi-terminal VSC-HVDC transmission system," in *Proc. IEEE Power Energy Soc. Gen. Meeting*, Denver, CO, USA, Jul. 2015, pp. 1–5.
[23] E. Barklund, N. Pogaku, M. Prodanovic, C. Hernandez-Aramburo, and T. C. Green, "Energy management in autonomous microgrid using stability-constrained droop control of inverters," *IEEE Trans. Power Electron.*, vol. 23, no. 5, pp. 2346–2352, Sep. 2008.
[24] A. Kirakosyan, E. F. El-Saadany, M. S. El Moursi, S. S. Acharya, and K. Al Hosani, "Control approach for the multi-terminal HVDC system for the accurate power sharing," *IEEE Trans. Power Syst.*, vol. 33, no. 4, pp. 4323–4334, Jul. 2018.
[25] T. L. Vandoorn, J. D. M. De Kooning, B. Meersman, and L. Vandevelde, "Improvement of active power sharing ratio of P/V droop controllers in low-voltage islanded microgrids," in *Proc. IEEE Power Energy Soc. Gen. Meeting*, Vancouver, BC, Canada, Jul. 2013, pp. 1–5.
[26] Y. Gu, X. Xiang, W. Li, and X. He, "Mode-adaptive decentralized control for renewable DC microgrid with enhanced reliability and flexibility," *IEEE Trans. Power Electron.*, vol. 29, no. 9, pp. 5072–5080, Sep. 2014.
[27] C. Wei, Y. Daopei, C. Jialin, W. Yongzhi, and Y. Yuxing, "The impact of line resistance on load sharing and an improved droop control of DC microgrid," in *Proc. 9th Int. Conf. Power Electron. ECCE Asia (ICPE-ECCE Asia)*, Seoul, South Korea, Jun. 2015, pp. 208–212.

YUCHAO LIU received the B.S. degree in electronic information engineering from the Harbin University of Science and Technology, Harbin, China, in 2011, and the M.S. degree in electrical engineering from the Harbin Institute of Technology, Harbin, in 2014, where she is currently pursuing the Ph.D. degree in electrical engineering. From 2017 to 2018, she was a Visiting Student with Imperial College London, U.K. Her research interests include control strategy and stability analysis of multi-terminal dc transmission.

TIM C. GREEN received the B.Sc. (Eng.) degree (Hons.) from Imperial College London, U.K., in 1986, and the Ph.D. degree from Heriot-Watt University, Edinburgh, U.K., in 1990. He is currently a Professor of electrical power engineering at Imperial College London, and the Director of the Energy Futures Lab with a role of fostering interdisciplinary energy research across the university. His research is focused on using the flexibility of power electronics to further the decarbonization of electricity systems by easing the integration of renewable sources and EV charging. In HVDC, he has contributed converter designs that strike improved tradeoffs between power losses, physical size, and fault handling. In distribution systems, he has pioneered the use of soft open points and the study of stability of grid-connected inverters. He is a Chartered Engineer in U.K. and a Fellow of the Royal Academy of Engineering.

JIAN WU received the B.S., M.S., and Ph.D. degrees in electrical engineering from the Harbin Institute of Technology (HIT), Harbin, China, in 2001, 2003, and 2007, respectively. In 2007, he joined the Department of Electrical Engineering, HIT, as a Lecturer. His research interests include power quality, VSC-MTDC, monitoring schemes for distribution networks, and multi-level converters.

KUMARS ROUZBEHI (S'13–M'16–SM'16) received the Ph.D. degree in electric energy systems from the Technical University of Catalonia (UPC), Barcelona, Spain. Prior to his Ph.D. program, he was with the faculty of Electrical Engineering as academic staff, Islamic Azad University (IAU), from 2004 to 2011. In parallel with teaching and research at the IAU, he was the CEO of Khorasan Electric and Electronics Industries Researches Company from 2004 to 2010. From 2017 to 2019, he was an associate professor at the Loyola Andalucía University. In 2019, he joined the department of systems and automatic engineering, University of Seville. He holds a patent in AC grid synchronization of voltage source power converters and has authored and co-authored more than 50 technical books, book chapters, journal papers, and technical conference proceedings.

Dr. Rouzbehi has been a member of the Amvaje-e-bartar Policy Making Committee and has been serving as an Editor since 2006, and as an Associate Editor in IET High Voltage, and IET Energy Systems Integration since 2018. He was the recipient of the Second Best Paper Award 2015 from the IEEE Power Electronics Society from the IEEE JOURNAL OF EMERGING AND SELECTED TOPICS IN POWER ELECTRONICS. He has been a TPC Member of the International Conference on Electronic, Communication, Control, and Power Engineering (IEEE-ECCP) since 2014 and a Scientific Board Member of the (IEA) International Conference on Technology and Energy Management since 2015.

ALI RAZA received the B.S. and M.Sc. degrees in electrical engineering from the University of Engineering and Technology, Lahore, Pakistan, in 2010 and 2013, respectively, and the Ph.D. degree in electrical engineering from the Harbin Institute of Technology, Harbin, China, in 2016. He is currently an Assistant Professor with the Department of Electrical Engineering, The University of Lahore, Pakistan. His research interests include operation and control of M-VSC-HVDC, including its effects on power systems, integration of distributed generation systems to the grid, resonance analysis and oscillation damping, and topological evaluation of MTDC transmission systems for large offshore wind power plants.

DIANGUO XU (M'97–SM'12–F'17) received the B.S. degree in control engineering from Harbin Engineering University, Harbin, China, in 1982, and the M.S. and Ph.D. degrees in electrical engineering from the Harbin Institute of Technology (HIT), Harbin, in 1984 and 1989, respectively. In 1984, he joined the Department of Electrical Engineering, HIT, as an Assistant Professor. Since 1994, he has been a Professor with the Department of Electrical Engineering, HIT. He was an Assistant President of HIT, from 2010 to 2014, where he has been a Vice President, since 2014. His research interests include renewable energy generation technology, M-VSC-HVDC transmission systems, power quality mitigation, and speed sensorless vector controlled motor drives. He serves as the Chairman of the IEEE Harbin Section. He is an Associate Editor of the IEEE TRANSACTIONS ON INDUSTRIAL ELECTRONICS.